

Optical microscopy of single ions and morphological inhomogeneities in Sm-doped CaF₂ thin films

R. Rodrigues-Herzog,* F. Trotta, and H. Bill†

Department of Physical Chemistry, University of Geneva, 30 quai Ernest-Ansermet, CH-1211 Geneva 4, Switzerland

J.-M. Segura and B. Hecht

Laboratory of Physical Chemistry, Swiss Federal Institute of Technology, ETH-Z, CH-8092 Zurich, Switzerland

H.-J. Güntherodt

Department of Physics and Astronomy, University of Basel, Klingelbergstrasse 82, CH-4056 Basel, Switzerland

(Received 19 May 2000)

We have investigated the luminescence of CaF₂ thin films doped with very low concentrations of Sm²⁺ ions using scanning confocal optical microscopy at low temperatures. The film morphology was studied independently by atomic force microscopy. The Sm²⁺ ions are homogeneously distributed in the films and show photobleaching. Unexpectedly, on the film surface strongly luminescent small topographic features are observed that are found to contain Sm³⁺ by spectral analysis. The formation of Sm³⁺ is probably due to the presence of oxygen during film growth. In the lowest doped films on-off blinking behavior of isolated luminescent spots provides strong evidence for the first observation of single ions in a crystal.

I. INTRODUCTION

Optical spectroscopy is an important tool in the characterization of photoactive impurities in inorganic crystals. However, most conventional spectroscopic techniques represent measurements of ensemble averages whereby different material sites are simultaneously probed and average responses are recorded. Different ionic impurity sites in the activated inorganic crystal experience different local fields so that each impurity site has a different local resonance frequency. By probing all these sites simultaneously the distribution in energies leads to a broadened electronic spectrum. As a consequence important information about the different sites often escapes notice. Experiments that remove this inhomogeneous broadening can reveal not only the underlying spectrum but also lead to important information about the chemical origin of the different environments. Typical methods for studying such inhomogeneous systems are frequency-resolved methods such as spectral hole burning^{1,2} and fluorescence line narrowing,² which employ narrow-frequency light sources to isolate individual energy sites. However, these sites still include a large number of impurities and thus cannot completely avoid ensemble averaging.

In the last years, advances in instrumentation have allowed the isolation and detection of few atomic particles and molecules in different materials. Many studies have been performed with optical detection of single molecules,³⁻⁶ single defects in crystals,⁷ single atoms in atomic beams,⁸ and single ions in electromagnetic traps.⁹ The observation of single ionic impurities in a crystal lattice has been proposed by Süssle *et al.*¹⁰ Based on measurements of the spatial variations of the luminescence intensity, Lange *et al.*¹¹ have pointed out the possibility to perform optical experiments with a small number of Sm²⁺ ions in bulk CaF₂. The photophysical parameters of the ions in this system indicate their suitability for single-ion detection: absorption cross

section at 610 nm, $\sigma \approx 5 \times 10^{-18}$ cm², excited-state lifetime at 708 nm, $\tau \approx 2$ μ s, and luminescence quantum yield at 77 K, $\eta \approx 1$.^{12,13}

In this article we study the spatial and spectral distribution of the luminescence of a very small concentration of Sm²⁺ ions in CaF₂ thin films using scanning confocal optical microscopy (SCOM) at low temperatures. By using thin films, out-of-focus luminescence is eliminated, and, in the limit of very low concentrations, the number of ions in the detection volume can be tuned by varying the film thickness. The thin-film morphology was independently investigated by atomic force microscopy (AFM) in order to exclude the possibility that spatial variations in luminescence could originate from local changes in film thickness. The Sm²⁺ ions in thicker films are found to be homogeneously distributed and undergo photobleaching. Surprisingly, we also observe small strongly luminescent features in the films that exhibit the typical emission spectrum of Sm³⁺ ions in CaF₂. AFM topographs of the films show small raised structures that we identify with the bright features observed in SCOM images. Thinner films with lower ion concentration hardly exhibit any raised topographic structures. The homogeneous Sm²⁺ luminescence in these samples is replaced by dimly emitting spots displaying a blinking behavior characteristic for single particles. These results strongly support that we have observed the luminescence of single ions in an inorganic crystal.

II. EXPERIMENT

CaF₂ thin films doped with very low concentrations of samarium (Sm²⁺) impurity ions were grown in a home-built molecular beam epitaxy (MBE) apparatus.¹⁴⁻¹⁶ Source crystals of CaF₂ doped with a desired concentration of Sm²⁺ were evaporated from a high-temperature effusion cell and deposited on a pure CaF₂ (111) cleaved crystal substrate. The source crystals used for evaporation were prepared from

ultrapure CaF_2 (Aldrich) and SmF_3 (Cerac 99.8% purity) in a Bridgman furnace (oxygen partial pressure $<10^{-7}$ Pa). The strongly reducing conditions present in the Bridgman apparatus favored the incorporation of Sm^{2+} ions in the crystals. To obtain very low doping levels, successively grown source crystals were systematically diluted by using material from the previously grown crystal as a dopant, with the sequence 10^{-3} , 10^{-6} , 10^{-9} , 10^{-10} , 10^{-11} , 10^{-12} (mol/mol). Two to three melting-crystallization cycles were realized each time to ensure a homogeneous impurity distribution. The films were grown with a typical MBE deposition rate of 0.03 nm/s that was monitored by a quartz microbalance. After growth, the films were cooled to room temperature at $1^\circ\text{C}/\text{min}$ in order to minimize thermally induced mechanical stress. The estimated residual concentration of O_2 in the machine during film growth was $\approx 10^{-7}$ Pa.

Films were grown with a thickness of 240 (sample A), 1000 (sample B), and 1500 nm (sample C). The thickness was determined by AFM measurements at the sample edge. The Sm^{2+} nominal doping concentration was 10^{-12} mol/mol (0.02 ions/ μm^3) for sample A and 10^{-10} mol/mol (2.0 ions/ μm^3) for samples B and C. However, at this level of concentration, nonintentional doping by residual Sm^{2+} present in the MBE apparatus cannot be excluded. The substrate temperature was kept at 600°C during growth for all films except for film C, which was grown at 300°C . A cleaved undoped CaF_2 bulk substrate was used as a blank sample (D).

The Sm impurity ions occur as Sm^{2+} and/or Sm^{3+} ions, depending on the growth conditions and whether or not the crystals are hydrolyzed after growth. It is therefore important to compare the emission spectra of Sm^{2+} and Sm^{3+} in CaF_2 in order to analyze the luminescence of our low-level doped films. We thus prepared in our Bridgman furnace two additional $\text{CaF}_2:\text{Sm}^{2+}$ single crystals with higher doping concentrations. The first one (sample E) was grown with a doping concentration of 10^{-9} mol/mol Sm^{2+} . The second one (sample F), grown by adding 0.1% of SmF_3 , was hydrolyzed after growth at 900°C under water vapor during 6 h. Under this treatment the Sm^{2+} ions are oxidized into Sm^{3+} and thereby samarium-oxygen complexes are formed.¹⁷ Sample E is lightly green due to the predominant doping with Sm^{2+} ions. On the other hand, the hydrolyzed sample (F) is transparent and colorless, showing the virtually exclusive presence of Sm^{3+} ions in the crystal.

Luminescence spectra of the doped single crystals (samples E and F) were recorded on a home-built computer-controlled spectrometer at room temperature and at $T=100$ K. The luminescence was analyzed at a right angle with the aid of a double monochromator and a photon-counting system. To resonantly excite the Sm^{2+} ions, the 632.8 nm line of a He-Ne laser was used, which is close to a $4f-5d$ absorption line of Sm^{2+} in CaF_2 . Furthermore, for both samples luminescence spectra with excitation at 488 nm were recorded.

The emission spectrum of sample E at $T=100$ K is shown in Fig. 1(a). The highest narrow peak at 708 nm corresponds to the zero-phonon line of the $A_{1u}(4f^55d) \rightarrow T_{1g}(4f^6)$ transition of Sm^{2+} ions in CaF_2 .¹³ The shoulder towards lower energies is due to the coupling of this transition to phonons

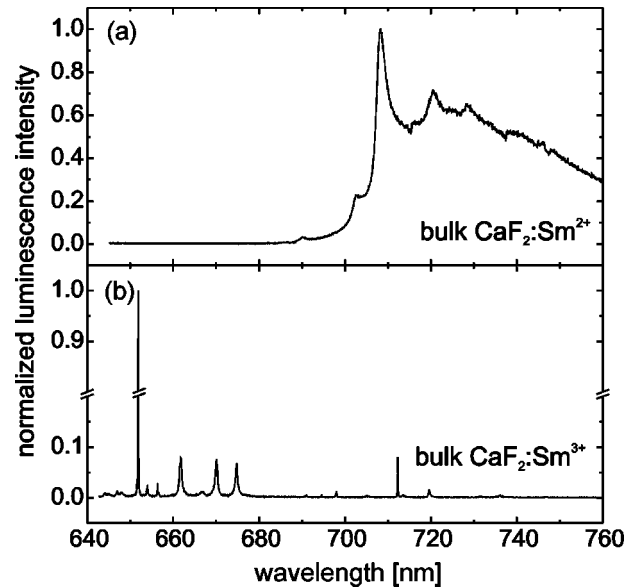


FIG. 1. Luminescence spectra of (a) a $\text{CaF}_2:\text{Sm}^{2+}$ bulk crystal (sample E) at $T=100$ K recorded at an excitation wavelength $\lambda_{\text{exc}}=632.8$ nm and of (b) a $\text{CaF}_2:\text{Sm}^{3+}$ bulk crystal (sample F) at $T=100$ K and $\lambda_{\text{exc}}=488$ nm.

in the crystal. Figure 1(b) shows the luminescence spectrum of sample F at $T=100$ K. A characteristic spectrum of Sm^{3+} in CaF_2 is observed.

The film morphology was studied using AFM. The experiments were performed in noncontact mode with a commercial system (TopoMetrix, Explorer TMX2000). Topography images were recorded using microfabricated silicon cantilevers with a spring constant of ~ 42 N m^{-1} . To exclude tip artifacts, control measurements were performed with different probe tips. Images of 100, 20, 10, 2, and $1\ \mu\text{m}$ scan width were recorded for all films.

In order to study the optical properties of the low-doped CaF_2 films, a home-built SCOM working at variable temperatures was employed, described extensively in Ref. 18. The excitation light is provided by a single-mode ring dye laser. The excitation wavelength of 592 nm was monitored by a wavemeter. This excitation energy is on the blue edge of a $4f-5d$ absorption line of Sm^{2+} in CaF_2 . The intensity was power-stabilized to typically $400\ \mu\text{W}$. The excitation beam was reflected by a dichroic mirror (50% transmission at 645 nm) into the cryostat, where it was focused to the sample by a microscope objective. The same objective was used to collect the sample emission. The luminescence signal was transmitted through the dichroic mirror and was focused onto a single-photon-counting avalanche photodiode (SPAD) acting as the detection pinhole. The back-reflected stray laser light from the sample surface and from the cryostat windows was cut off spectrally by the combination of a notch filter and two colored glass filters (optical density of 1 at 612 nm) and spatially using an aperture. Confocal images were recorded at room ($T=300$ K), liquid nitrogen ($T=77$ K), and superfluid helium ($T=1.8$ K) temperatures. In this configuration the optical resolution of the microscope was typically $1\ \mu\text{m}$.

For spectral analysis, the collected luminescence was deflected to a spectrometer (Jobin Yvon-Spex 270M, 0.27 m focal length) coupled to a charge-coupled device (liquid-

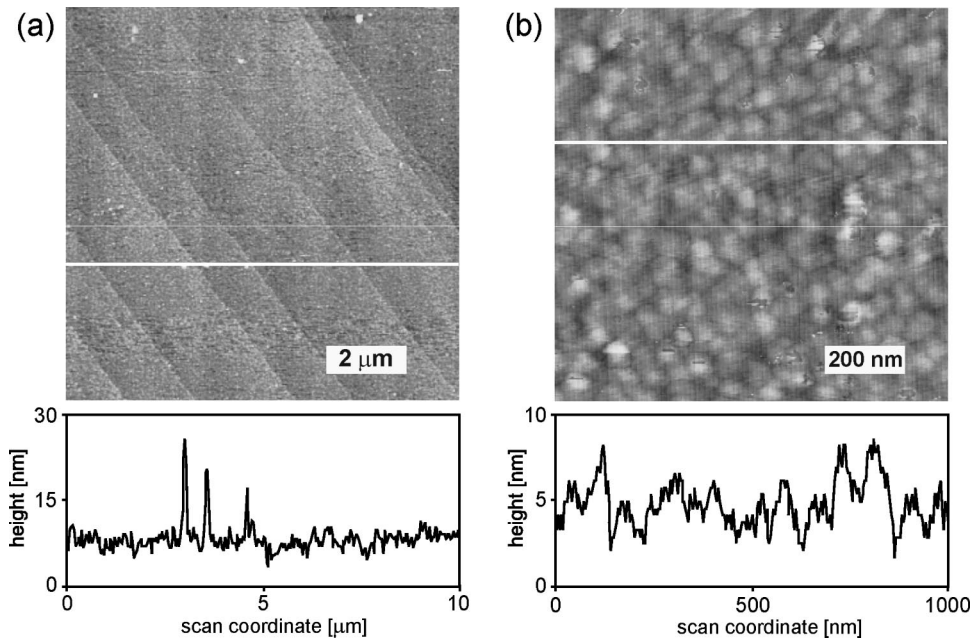


FIG. 2. AFM images of film A with scan areas of (a) 10×10 and (b) $1 \times 1 \mu\text{m}^2$. The surface profile along the line marked on the images is plotted below the respective image.

nitrogen cooled, 1024×256 pixels, $27 \mu\text{m}$ pixel size, quantum efficiency of 50%). The spectrometer is equipped with a 1200 grooves/mm holographic grating achieving a spectral dispersion of 3.1 nm/mm. Due to the absence of a pinhole in the detection path, the spatial resolution was slightly worse in the sample plane and much poorer along the optical axis as compared to the SPAD configuration. For each spectrum, the dark noise was subtracted and the spectrum was divided by the nonlinear characteristics of the dichroic mirror.

III. RESULTS AND DISCUSSION

A. Morphological inhomogeneities

Figure 2 shows typical AFM images obtained for sample A (240 nm thickness) for (a) 10×10 and (b) $1 \times 1 \mu\text{m}^2$ scan areas. Below each image the surface profile along the marked

line is plotted. This film showed on a short length scale a root-mean-square roughness of $R_{\text{rms}} = 1.4 \text{ nm}$ (Ref. 19) and in the micrometer range a very smooth topography. As can be seen from Fig. 2(b), the film consists of small grains ($\approx 4 \text{ nm}$ in height and 60 nm in width). The steps observed in Fig. 2(a) arise from the cleaved CaF_2 substrate. In the same image there are a few small raised structures up to 20 nm in height. Three of them are highlighted in the corresponding line profile.

Figure 3 depicts AFM images of sample B (1000 nm thickness) for different scan areas. Figure 3(a) shows a smooth surface with many of the raised structures already observed in sample A. They are mainly found at substrate steps or scratches. Comparison of Fig. 3 and Fig. 2(a) shows that the number of raised structures and their size increase with film thickness. For film B, their sizes range from hun-

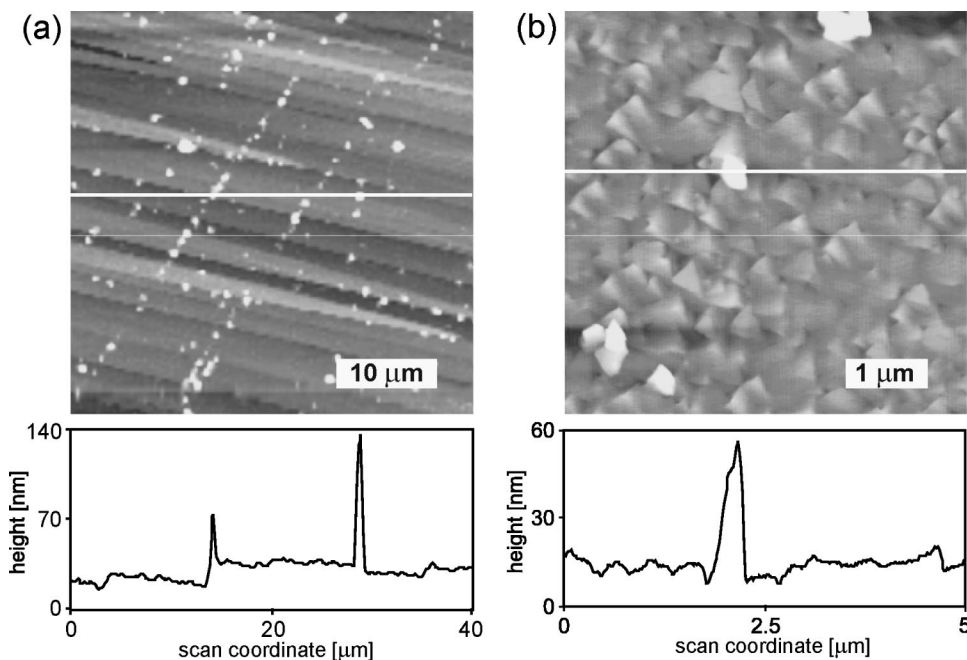


FIG. 3. AFM images of film B with scan areas of (a) $40 \times 40 \mu\text{m}^2$ and (b) $5 \times 5 \mu\text{m}^2$. The surface profile along the line marked on the images is plotted below the respective image.

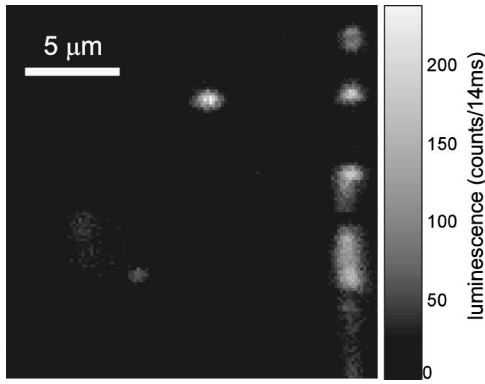


FIG. 4. Confocal image obtained for film B ($2.0 \text{ ions}/\mu\text{m}^3$) at $T=77 \text{ K}$, excitation wavelength $\lambda_{\text{exc}}=592.1 \text{ nm}$, and excitation intensity $I_{\text{exc}}=5 \text{ kW}/\text{cm}^2$.

dreds of nanometers to few microns in width and up to 200 nm in height. At the same time the grains that compose the thicker film exhibit larger sizes ($\approx 10 \text{ nm}$ in height and 300 nm in width) than in film A, while the surface roughness remains constant ($R_{\text{rms}}=1.4 \text{ nm}$). The grains have the shape of deformed rhombo-octahedra, indicating dominant growth along the $\langle 111 \rangle$ directions [Fig. 3(b)].

The luminescence of the Sm^{2+} -doped CaF_2 thin films was investigated using SCOM. Figure 4 shows a typical confocal image obtained for sample B at $T=1.8 \text{ K}$ where bright features on top of a structureless luminescence signal are observed. Some of these bright features are located along a straight line. This is similar to the behavior observed for the raised structures in the AFM image of film B [Fig. 3(a)]. Based on the fact that we have observed similar patterns in the optical and topographical images of several samples, we conclude that the bright features correspond to the raised structures.

The emission spectrum recorded at the position of a bright feature of sample B at $T=77 \text{ K}$ is plotted in Fig. 5(a). It is composed of two traces recorded consecutively, marked with roman letters I and II indicating the sequence. Spectrum I ($>700 \text{ nm}$) is very similar to the spectrum of sample E (Sm^{2+} in bulk CaF_2) shown in Fig. 1(a). The peak around 706 nm is identified with the zero-phonon emission line of the Sm^{2+} ions in CaF_2 . It also exhibits a shoulder towards lower energies corresponding to the phonon wing. However, the fine structure observed in the phonon wing of the bulk spectrum [Fig. 1(a)] is not observed in the film. This can be attributed to the fact that the phonon scattering mechanisms as well as the phonon spectrum in the film are different from the bulk crystal due to the higher disorder in the film.²⁰

Two other peaks at 663 and 678 nm can be clearly distinguished in trace II of the spectrum in Fig. 5(a). Peaks at similar wavelengths between 630 and 690 nm are found in the spectrum of sample F [Sm^{3+} in bulk CaF_2 , Fig. 1(b)] which are characteristic for the Sm^{3+} transitions in CaF_2 single crystals.

Figure 5(b) shows the spectrum (traces I and II) at the position of a bright feature of sample B now at $T=1.8 \text{ K}$. The spectrometer entrance slit was wider for trace II ($<700 \text{ nm}$) explaining the intensity translation between the traces. Again the Sm^{2+} zero-phonon line around 706 nm is present, but at this lower temperature it becomes much nar-

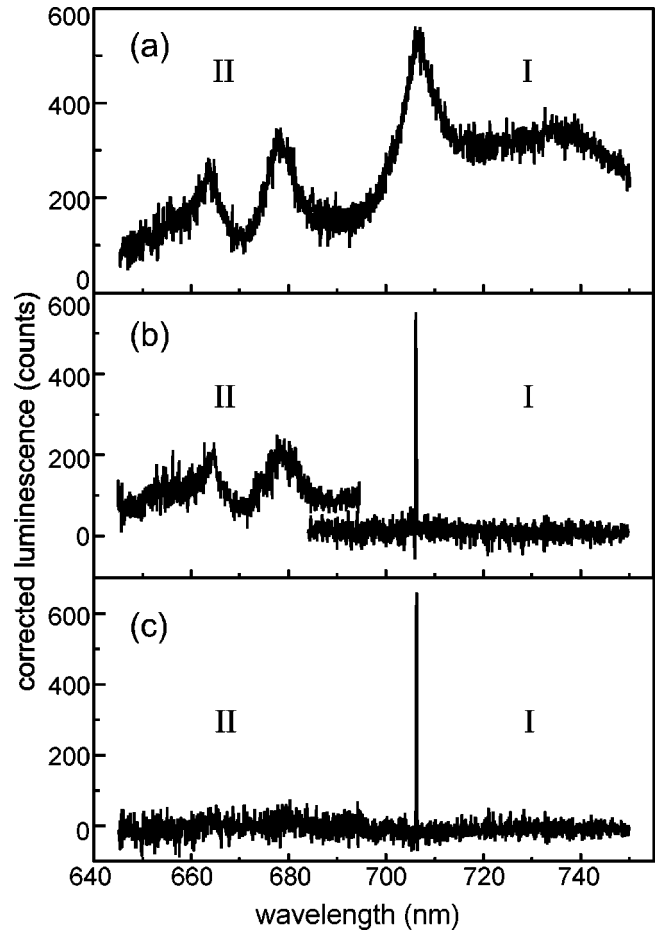


FIG. 5. Consecutively recorded luminescence spectra (I and II indicate the sequence) at the position of a bright luminescent feature of film B at (a) $T=77 \text{ K}$, $I_{\text{exc}}=100 \text{ kW}/\text{cm}^2$, integration time 60 s , resolution 3.1 nm and at (b) $T=1.8 \text{ K}$, $I_{\text{exc}}=40 \text{ kW}/\text{cm}^2$, integration time 120 s , resolution 1.6 nm . (c) Emission spectra of the structureless luminescence at $T=1.8 \text{ K}$, $I_{\text{exc}}=40 \text{ kW}/\text{cm}^2$, integration time 120 s , resolution 1.6 nm . Excitation wavelength for all spectra $\lambda_{\text{exc}}=592.2 \text{ nm}$.

rower and the phonon wing disappears. In contrast, the emission linewidth of the transitions at 663 and 678 nm (trace II) almost remains the same at $T=77$ and 1.8 K . This is a typical behavior for Sm^{3+} transitions in CaF_2 . The Sm^{3+} emission lines originate from $f-f$ transitions that have an almost temperature-independent Debye-Waller factor close to 1 ($T \leq 300 \text{ K}$).²¹ On the other hand, the Sm^{2+} bands, basically corresponding to $f-d$ transitions, show a pronounced temperature dependence. This finding, together with the line positions, strongly supports that the emission lines at 663 and 678 nm are due to the presence of Sm^{3+} in the bright features. The Sm^{3+} ions present a high number of f levels in their energy configuration and these levels are very close in energy to each other.²² In consequence they show a strong interaction with the local crystal field. Thus the $f-f$ transitions of Sm^{3+} ions exhibit widths and positions that are very dependent on the environment.²³ This explains the broad linewidths of the emission lines at 663 and 678 nm .

To compare the luminescence at the position of a bright feature with the structureless luminescence elsewhere in the

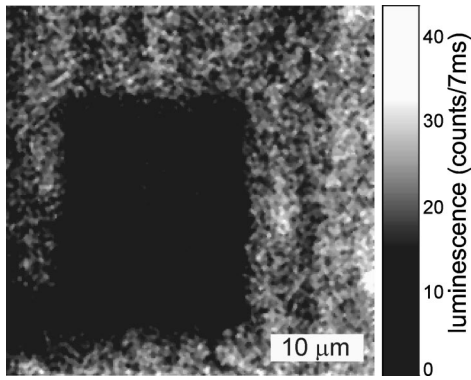


FIG. 6. Confocal image of a region free of bright luminescent features on film B obtained from two consecutive scans. First an area of $20 \times 20 \mu\text{m}^2$ was scanned. After that a $40 \times 40 \mu\text{m}^2$ image was recorded that included the previously scanned area. $T = 77 \text{ K}$, $\lambda_{\text{exc}} = 592.2 \text{ nm}$, and $I_{\text{exc}} = 20 \text{ kW/cm}^2$.

image of Fig. 4, we have plotted in Fig. 5(c) a spectrum recorded at a location far from any bright feature. The Sm^{2+} zero-phonon line at 706 nm is also observed here. The intensity of this line was found to be fairly constant everywhere in the film, indicating a homogeneous distribution of the Sm^{2+} ions. However, the Sm^{3+} bands—which are found in the spectrum of a bright feature [Fig. 5(b)]—are not present in the spectrum of the structureless luminescence. Taking into account the homogeneous distribution of the Sm^{2+} ions in the film and the limited optical resolution along the optical axis when recording spectra, we believe that the Sm^{2+} bands in the spectra taken at positions of bright features [Figs. 5(a) and (b)] actually originate from the underlying film and not from the raised structures on top of the film. Thus the raised structures are probably doped exclusively with Sm^{3+} ions.

The presence of Sm^{3+} in the films is intrinsically related to the formation of the raised structures. In analogy with the Sm^{3+} generation mechanism mentioned for sample F, we suggest here the formation of samarium-oxygen complexes during film growth. Due to the presence of residual oxygen in the MBE apparatus, part of the Sm^{2+} can be oxidized to

Sm^{3+} during film preparation. These trivalent rare-earth impurities are then incorporated into the CaF_2 lattice by substituting divalent alkaline-earth-metal ions.²⁴ Here, the charge compensation is probably obtained by the clustering of trivalent Sm^{3+} with the residual oxygen in the MBE machine. This is possible due to the high mobility of the ions on the film surface during growth at a substrate temperature of 600°C . In the images, the raised structures are very often observed near a scratch or substrate step on the film surface. Samarium-oxygen clusters are probably trapped by these imperfections and accumulate. This explains the positioning of the raised structures preferentially along straight lines following substrate imperfections.

The fact that the ions have a high mobility during film growth is demonstrated by the following observation. By varying the axial distance of the microscope objective relative to the sample, one can obtain depth profiles of the luminescence and thus of the ion concentration. Such measurements on sample B, grown at a substrate temperature of 600°C , show that luminescence emission of the Sm^{2+} ions is observed not only in the film but also in the CaF_2 substrate. Consequently, the impurity ions diffuse into the bulk CaF_2 substrate. In contrast, no luminescence in the substrate was observed for film C grown at similar conditions except a lower substrate temperature of 300°C . This result is compatible with the strong temperature dependence of the ion mobility. Interestingly, neither bright features nor Sm^{3+} luminescence was ever observed in a substrate. This also confirms that the formation of the bright features takes place exclusively on the film surface.

The Sm^{2+} ions in the films could be photobleached by the excitation laser light as illustrated in Fig. 6. To obtain this confocal image, first a region of film B without bright features was selected, and a smaller quadratic area was scanned. Then the scan range was increased and the image was recorded. During the first scan, the Sm^{2+} ions are photobleached leading to a lower emission intensity in this area compared to the rest of the image. A possible explanation for the bleaching of the Sm^{2+} ions is their photo-oxidation into trivalent samarium.^{1,25}

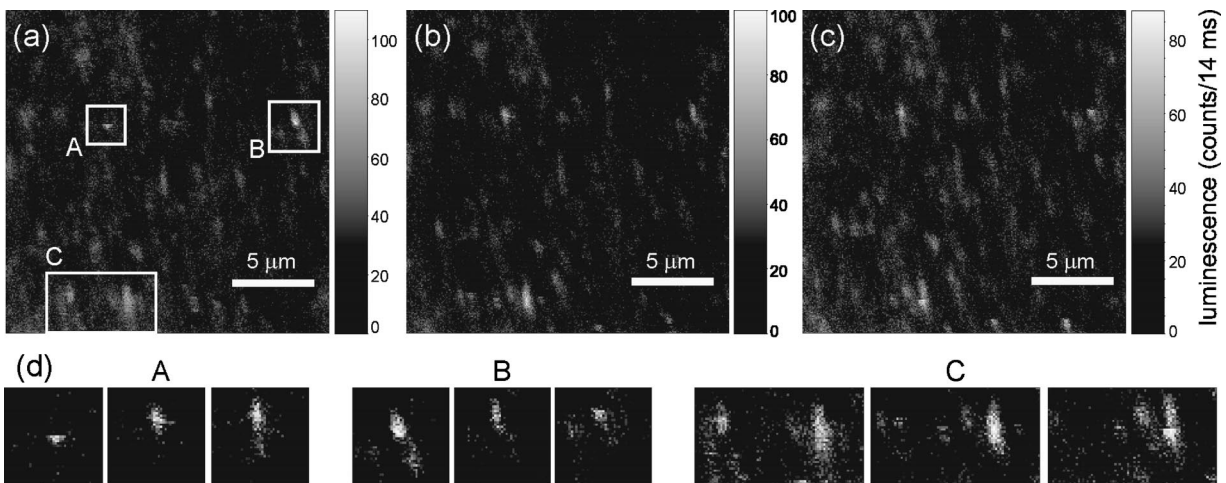


FIG. 7. Three confocal images of the same area of film A ($0.02 \text{ ions}/\mu\text{m}^3$) recorded consecutively at $T = 77 \text{ K}$, $\lambda_{\text{exc}} = 592.2 \text{ nm}$, and $I_{\text{exc}} = 40 \text{ kW/cm}^2$. The spots marked by rectangles A, B, and C in (a) show an on-off blinking behavior: the spots show dark stripes or truncated shapes that often differ from shapes observed in the consecutive images (b) and (c). (d) Evolution of the spot shapes (magnifications of A, B, and C) between the consecutive images (a), (b), and (c).

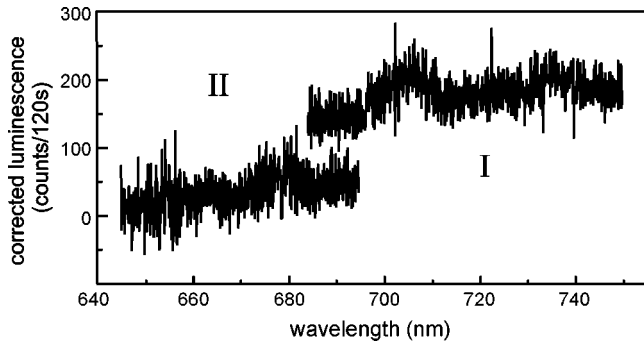


FIG. 8. Consecutively recorded luminescence spectra (I, II) of film A at $T=77$ K, $\lambda_{\text{exc}}=592.2$ nm, $I_{\text{exc}}=40$ kW/cm², and a resolution of 3.1 nm. Each spectrum was recorded while scanning the same area as for Fig. 7.

B. Single ions

A different luminescence emission behavior was observed for the lowest doped film A, as depicted in Fig. 7, which shows three confocal images of sample A (0.02 ions/ μm^3). These images were recorded consecutively. Instead of the structureless luminescence present in the confocal images of sample B, numerous small dim spots are observed here. Careful analysis of the spots marked by rectangles in the image in Fig. 7(a) shows that the spot shape can vary between consecutive images: Often complete spots change to truncated spots or to spots with intermittent dark lines and vice versa. Many other spots in the images, which are not marked, display the same behavior. Examples of such fluctuations are highlighted in Fig. 7(d). These shapes are a typical signature of on-off blinking often observed in single-particle experiments.³⁻⁶ The special spot shapes originate from the fact that, in SCOM, images are scanned horizontally, line by line, from bottom to top. While being scanned the single ions can undergo photoinduced transitions to metastable dark-states. Depending on the dark-state lifetime the respective spot exhibits dark lines or even becomes truncated in the confocal image. In some cases truncated spots do not appear in the consecutive images, corresponding to single-step photobleaching. The typical peak luminescence count rate of isolated spots was about 3600 s⁻¹, which corresponds to an actual luminescence rate of 1.2×10^5 s⁻¹ using the $\approx 3\%$ detection efficiency of the setup.¹⁸ This is compatible with the expected saturation count rate of 5×10^5 s⁻¹ for a single ion, derived from the excited-state lifetime.

Due to the extremely low luminescence count rates in film A and the fast photobleaching, spectra at $T=77$ K have only been recorded while scanning the confocal image of Fig. 7

and not at a fixed position on the sample. The resulting consecutively recorded spectra I and II are shown in Fig. 8. Spectrum I shows a weak band around 706 nm, which can be assigned to the Sm²⁺ zero-phonon line. This strongly supports that the spots observed in Fig. 7 are due to Sm²⁺ ions. Spectrum II only shows background luminescence. The offset between spectra I and II is most probably due to photobleaching after recording the first spectrum (I).

To be sure that the bright structures and the blinking spots are only present in the films, we further investigated the blank CaF₂ crystal (sample D) using SCOM. No structure could be observed in confocal images. The count rates were constant and very low, corresponding to the system background. The dimly blinking spots were observed only in the confocal image of the lowest doped film and are related intrinsically to the film luminescence. The spectrum of the emission and the on-off blinking behavior provide strong evidence that the spots observed in Fig. 7 are single Sm²⁺ ions.

IV. CONCLUSIONS

We have investigated the spatial and spectral properties of the luminescence and the topography of CaF₂ thin films doped with a very low concentration of Sm²⁺ ions. In thicker films, the Sm²⁺ ions are found to be homogeneously distributed. However, we observe morphological inhomogeneities that appear as bright luminescent features in optical images and raised structures in AFM topography, respectively. These inhomogeneities contain Sm³⁺ ions and are formed during film growth at imperfections of the substrates. Thinner films with lower ion concentration hardly exhibit any raised topographic structures. The homogeneous luminescence in these films breaks up into weakly emitting spots exhibiting on-off blinking behavior and single-step photobleaching, and showing the characteristic spectrum of Sm²⁺. These observations provide strong evidence for optical detection of single ions in an inorganic crystal.

Note added. After submission of this paper, a paper appeared²⁶ that reports blinking luminescence of Eu³⁺ in Y₂O₃ nanocrystals.

ACKNOWLEDGMENTS

Thanks are expressed to V. Thommen for supporting the AFM experiments. We are also very grateful to H. Heinzelmann, D. Pohl, M. Freiland, R. Eckert, and M. Schnieper for valuable discussions. Professor U.P. Wild is gratefully acknowledged for continuous interest and support. Part of the project was funded by the Swiss National Science Foundation (NFP 36) and ETH Zürich.

*Also at Department of Physics and Astronomy, University of Basel, Klingelbergstr. 82, CH-4056 Basel, Switzerland.

†Email: Hans.Bill@chiphys.unige.ch

¹*Persistent Spectral Hole-Burning: Science and Applications*, Topics in Current Physics **44**, edited by W.E. Moerner (Springer-Verlag, Berlin, 1988).

²*Zero-Phonon Lines and Spectral Hole Burning in Spectroscopy and Photochemistry*, edited by O. Sild and K. Haller (Springer-Verlag, Berlin, 1988).

³*Single-Molecule Optical Detection, Imaging and Spectroscopy*, edited by T. Basché, W.E. Moerner, M. Orrit, and U.P. Wild (VCH, Weinheim, 1997).

⁴X.S. Xie and J.K. Trautman, *Annu. Rev. Phys. Chem.* **49**, 441 (1998).

⁵W.E. Moerner and M. Orrit, *Science* **283**, 1670 (1999).

⁶P. Tamarat, A. Maali, B. Lounis, and M. Orrit, *J. Phys. Chem. A* **104**, 1 (2000).

⁷A. Gruber, A. Dräbenstedt, C. Tietz, L. Fleury, J. Wrachtrup, and

- C. von Borczyskowski, *Science* **276**, 2012 (1997).
- ⁸H.J. Kimble, M. Dagenais, and L. Mandel, *Phys. Rev. Lett.* **39**, 692 (1977).
- ⁹F. Diedrich and H. Walther, *Phys. Rev. Lett.* **58**, 203 (1987).
- ¹⁰K.E. Süsse, W. Vogel, D.G. Welsch, and B. Wilhelmi, *Opt. Commun.* **28**, 389 (1979).
- ¹¹R. Lange, W. Grill, and W. Martienssen, *Europhys. Lett.* **6**, 499 (1988).
- ¹²W. Kaiser, C.G.B. Garrett, and D.L. Wood, *Phys. Rev.* **123**, 766 (1961).
- ¹³D.L. Wood and W. Kaiser, *Phys. Rev.* **126**, 2079 (1962).
- ¹⁴A. Monnier, M. Schnieper, R. Jaaniso, and H. Bill, *Radiat. Eff. Defects Solids* **135**, 253 (1995).
- ¹⁵A. Monnier, M. Schnieper, R. Jaaniso, and H. Bill, *J. Appl. Phys.* **82**, 536 (1997).
- ¹⁶M. Schnieper, F. Trotta, S. Bersier, and H. Bill, *Appl. Phys. Lett.* **75**, 40 (1999).
- ¹⁷F. Deyhimi and H. Bill, *J. Solid State Chem.* **43**, 181 (1982).
- ¹⁸J.-M. Segura, A. Renn, and B. Hecht, *Rev. Sci. Instrum.* **71**, 1706 (2000).
- ¹⁹ $R_{\text{rms}} = [(1/N)\sum_{i=1}^N (z_i - \bar{z})^2]^{1/2}$, and $\bar{z} = (1/N)\sum_{i=1}^N z_i$, where z_i is the intensity per pixel and N is the total number of pixels in the AFM image.
- ²⁰S. Alexander and R. Orbach, *J. Phys. (France) Lett.* **43**, L-625 (1982).
- ²¹K. Rebane, *Impurity Spectra of Solids* (Plenum Press, New York, 1970).
- ²²B.R. Judd, *Operator Techniques in Atomic Spectroscopy* (McGraw-Hill, New York, 1963).
- ²³R. Jaaniso, H. Hagemann, and H. Bill, *J. Phys. Chem.* **101**, 10 323 (1994).
- ²⁴W. Hayes, *Crystals with the Fluorite Structure* (Clarendon Press, Oxford, 1974).
- ²⁵R.M. Macfarlane and R.M. Shelby, *Opt. Lett.* **9**, 533 (1984).
- ²⁶M.D. Barnes, A. Metha, T. Thundat, R.N. Bhargava, V. Chhabra, and B. Kulkarni, *J. Phys. Chem. B* **104**, 6099 (2000).